Nanoscale Horizons

ROYAL SOCIETY OF CHEMISTRY

COMMUNICATION

View Article Online
View Journal | View Issue

Cite this: *Nanoscale Horiz.*, 2025, **10**, 2953

Received 25th April 2025,
Accepted 7th August 2025

DOI: 10.1039/d5nh00271k

rsc.li/nanoscale-horizons

Direct kneading of thermo-softening pulp towards producing sustainable tough composites of wood nanocellulose and polycaprolactone

Masahiro Kasamatsu, [a] Shun Ishioka, *[ba] Noriyuki Isobe, [ca] Katsunori Kimoto, [c] Satoshi Okada, [d] Yohsuke Goi, [e] Shuji Fujisawa [a] and Tsuguyuki Saito *[a]

Cellulose nanofibre (CNF)-reinforced plastics were prepared by direct kneading of polycaprolactone (PCL) and a new type of pulp with thermo-softening nature. This thermo-softening pulp fully disintegrated into CNFs within a melted PCL through kneading, resulting in an increase in the strength and thermal stability of PCL while preserving its toughness.

[a] *Department of Biomaterial Sciences, Graduate School of Agricultural and Life Sciences, The University of Tokyo, 1-1-1 Yayoi, Bunkyo-ku, Tokyo 113-8657, Japan. E-mail: saitot@g.ecc.u-tokyo.ac.jp*

[b] *SANKEN (The Institute of Scientific and Industrial Research), The University of Osaka, 8-1 Mihogaoka, Ibaraki, Osaka, 567-0047, Japan. E-mail: s.ishioka@eco.sanken.osaka-u.ac.jp*

[c] *Biogeochemistry Research Center, Research Institute for Marine Resources Utilization (MRU), Japan Agency for Marine-Earth Science and Technology (JAMSTEC), 2-15 Natsushima-cho, Yokosuka, Kanagawa 237-0061, Japan*

[d] *Institute for Extra-cutting-edge Science and Technology Avant-garde Research (X-star), Japan Agency for Marine-Earth Science and Technology (JAMSTEC), 2-15 Natsushima-cho, Yokosuka, Kanagawa 237-0061, Japan*

[e] *Sustainable Materials R&D Group, Corporate R&D Department, Kyoto Central R&D Division, DKS Co. Ltd., 5 Ogawara-cho, Kisshoin, Minami-ku, Kyoto 601-8391, Japan*

New concepts

Direct kneading of wood pulp with melted polymers is an industrially feasible route for the production of cellulose nanofibre (CNF)-reinforced polymer composites. However, the resulting composites are often brittle due to the difficulty in disintegrating wood pulp into CNFs within a melted polymer matrix by kneading only. Herein, we report a new strategy for the fabrication of tough CNF-reinforced polymer composites *via* the energy- and time-efficient direct kneading of wood pulp. The novelty of our strategy lies in the fact that the pulp was chemically modified in advance to thermally soften at 100 °C or above. Polycaprolactone (PCL), which has a melting temperature lower than 100 °C, was selected as the polymer matrix. The thermo-softening pulp fully disintegrated into fine CNFs within the melted PCL matrix by kneading, resulting in a significant increase in the mechanical strength and thermal dimensional stability of PCL while preserving its high toughness. To be specific about the modification, anionic carboxy groups were formed at the interfaces of bundled CNFs within the pulp, followed by pairing these anions with organic cations dissociable below 100 °C. This modified pulp softens at 100 °C or above through self-diffusion of the dissociated cations at the inter-CNF interfaces.

Tsuguyuki Saito

It is my great pleasure to offer my congratulations on the 10th anniversary of Nanoscience Horizons. We are pleased to have the opportunity to contribute to this memorial collection with this article, along with our new research direction. Our first paper in Nanoscale Horizons was published in 2018. Following this, we were pleased to have the opportunity to publish two more articles in which we presented the latest findings from our research on nanocellulose. We are committed to making further contributions to this esteemed journal of nanoscale understanding in the next decade.

Introduction

Nanoscale particles with high aspect ratios, such as cellulose nanofibres (CNFs),[1,2] carbon nanotubes[3–5] and clay nanoplatelets,[6–8] are often employed as reinforcing fillers for polymers. The compounding of these particles into a polymer matrix, typically at a content of 10% w/w or less, can significantly enhance the mechanical and thermal properties of the polymer.[9] These polymer nanocomposites are characterized by high specific moduli, specific strengths and thermal dimensional stabilities and are thus expected to be suitable for use in automobiles,[10] electrical devices[11] and building materials.[12]

In recent years, CNFs have attracted attention as sustainable reinforcing fillers with high stiffness (130–150 GPa), high strength (2–3 GPa) and low thermal expansivity (6 ppm K^{-1}), contributing to a considerable reduction in the use of petroleum-based

plastics.[13–15] The lightweight nature of CNFs (1.6 g cm^{-3}) is also of advantage over other reinforcing fillers such as glass fibres (2.5 g cm^{-3}), carbon fibres (1.8 g cm^{-3}) and calcium carbonate (2.7 g cm^{-3}).[16] CNFs are produced *via* disintegration of wood pulp into the fine crystallite units of cellulose, which are histologically defined as microfibrils.[17] A successful process to homogeneously disperse CNFs in a polymer matrix for reinforcement is the solvent casting route.[2,18–20] However, this method requires a high energy input to produce CNFs in advance and is a time-consuming process to evaporate a large amount of organic solvent.[21] In addition, the resulting composites are typically produced in the form of thin films, which limits their applications.

Direct kneading is an industrially feasible route for the production of CNF-reinforced plastics. In this method, a pulp is directly added in the melt-kneading process of plastics using a twin-screw extruder, where the pulp is fibrillated into CNFs within the kneaded polymer matrix.[22–26] This process eliminates CNF production in advance and requires no solvents, thus reducing the time, energy and cost of manufacturing for CNF-reinforced plastics.[24] However, a high degree of fibrillation of a given pulp into fine CNFs is difficult to achieve in this kneading process because of strong interactions between cellulose crystallites in the pulp, leading to embrittlement of the resulting coarse CNF/polymer composites.

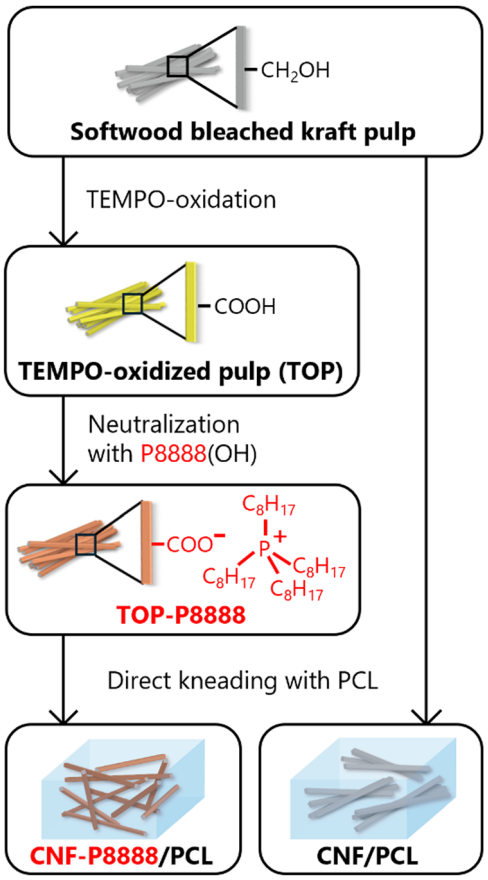

Fig. 1 Schematic illustration for preparation procedure of the CNF-P8888/PCL and CNF/PCL composites.

In this study, we developed a strategy to fabricate tough CNF-reinforced plastics *via* direct kneading through the use of thermo-softening pulp. Thermo-softening pulp was formed *via* the introduction of anionic functional groups on the surfaces of cellulose crystallites in the pulp, followed by pairing these anions with organic cations dissociable below 100 °C.[27,28] The thermo-softening property of the intercrystallite interfaces within the pulp enhanced the degree of fibrillation of CNFs within a melt-kneaded polymer, contributing to remarkable improvements in the mechanical and thermal properties of the polymer without reducing its toughness. Polycaprolactone (PCL) was chosen in this study as the polymer matrix. PCL is a biodegradable plastic, but its application is limited because of its low mechanical strength and low thermal dimensional stability.[29]

Results and discussion

In this study, thermo-softening pulp was utilized in the production of CNF-reinforced PCL through direct kneading (Fig. 1). Thermo-softening pulp was prepared from a 2,2,6,6-tetramethylpiperidine-1-oxyl (TEMPO)-oxidized softwood bleached pulp.[30] The sodium carboxylate groups in the TEMPO-oxidized pulp (TOP) were protonated using hydrochloric acid, followed by neutralization of the acid-type carboxy groups with tetraoctylphosphonium ($P8888^+$) hydroxide (refer to the SI for details). The resulting TOP-P8888 exhibits a thermo-softening nature (see Fig. S1).[27] The conversion ratio of acid-type carboxy groups to tetraoctylphosphonium

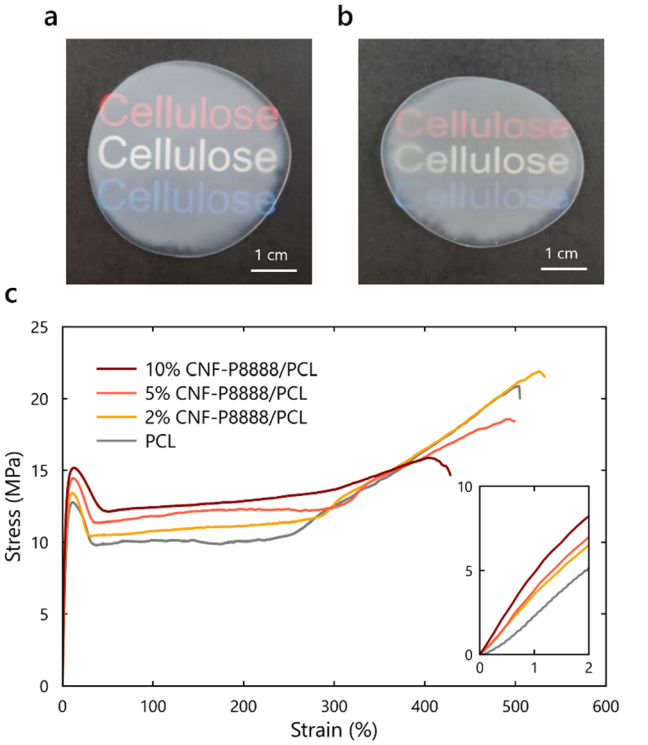

Fig. 2 CNF-P8888/PCL composite. Appearance of the (a) pristine PCL and (b) CNF-P8888/PCL composite at a 2% w/w CNF content. (c) Typical stress–strain curves of the pristine PCL and CNF-P8888/PCL composites with different CNF contents ranging from 2–10% w/w.

carboxylates was approximately 91%, as determined by Fourier transform infrared spectroscopy (FT-IR) (Fig. S2). The TOP-P8888 was then subjected to direct kneading with PCL using a twin-screw extruder, resulting in the production of CNF-P8888/PCL composites. PCL composites reinforced with pristine CNFs (CNF/PCL) were also prepared as a reference by directly kneading PCL and starting kraft pulp. Note that there existed no significant difference in fibre morphology between the starting kraft pulp, TOP and TOP-P8888 before kneading (Fig. S3), as illustrated as the CNF bundles in Fig. 1.

CNF-P8888/PCL composites with different CNF contents ranging from 2–10% w/w were prepared by direct kneading at 100 °C for 40 min (refer to Fig. S4 for the influence of the kneading time on the composite properties). After kneading, the pristine PCL and CNF-P8888/PCL composites were subjected to hot pressing at 2.5 MPa and 100 °C for 2 min to obtain flat sheets with a thickness of approximately 0.2 mm. The CNF-P8888/PCL composites showed no discolouration after kneading and were similar in appearance to pristine PCL (Fig. 2a and b). Discolouration is often observed during melt-kneading of plastics with CNFs due to their thermal degradation.[31] In this study, the melt-kneading was carried out at 100 °C, which is lower than the temperature at which TEMPO-oxidized CNFs start to discolor (~150 °C).

Fig. 2c shows typical stress–strain curves of the pristine PCL and CNF-P8888/PCL composites. Both PCL and its CNF-P8888 composites exhibited ductile tensile behaviour. At low strains, a linear elastic region followed by yielding was observed across all the samples. In the plateau region of plastic deformation, necking of the samples was initiated, and further elongation led to strain hardening.

The addition of 2% CNF-P8888 to PCL increased Young's modulus from 0.30 to 0.37 GPa, the yield strength from 12.5 to 13.4 MPa, the elongation at break from 503% to 542%, the strength at break from 18.7 to 22.1 MPa, and the toughness from 65 to 80 MJ m^{-3} (Table 1). Young's modulus and the yield strength further increased with increasing CNF content. The addition of 10% CNF-P8888 increased the modulus and yield strength to 0.51 GPa and 15.3 MPa, respectively, corresponding to enhancements of approximately 170% and 120%, respectively, compared with those of pristine PCL. The elongation and strength at break slightly decreased to 396% and 15.8 MPa, respectively. The toughness of the composites was accordingly preserved at 60 MJ m^{-3}, similar to the toughness of PCL.

Fig. 3a shows a comparison of the reinforcing functions of CNF-P8888 and pristine CNF for reference. Unlike those of PCL and CNF-P8888/PCL, no plateau region during plastic deformation was observed for the pristine CNF/PCL composites. The addition of pristine CNF to PCL increased Young's modulus, yield strength and strength at break to 0.52 GPa, 16.9 MPa, and 20.4 MPa, respectively (Table 1). The enhanced Young's modulus of the CNF/PCL composite was equivalent to the modulus

Table 1 Tensile properties of the pristine PCL and CNF-P8888/PCL composites

Sample	CNF content (% w/w)	Young's modulus (GPa)	Yield strength (MPa)	Elongation at break (%)	Strength at break (MPa)	Toughness (MJ m^{-3})
PCL	0	0.30 ± 0.11	12.5 ± 0.2	503 ± 78	18.7 ± 2.6	65 ± 14
CNF-P8888/PCL	2	0.37 ± 0.11	13.4 ± 0.3	542 ± 25	22.1 ± 1.2	80 ± 6
	5	0.41 ± 0.02	14.5 ± 0.3	493 ± 22	19.3 ± 0.8	73 ± 5
	10	0.51 ± 0.04	15.3 ± 0.6	396 ± 16	15.8 ± 0.6	60 ± 2
CNF/PCL	10	0.52 ± 0.01	16.9 ± 0.2	247 ± 35	20.4 ± 0.8	47 ± 5

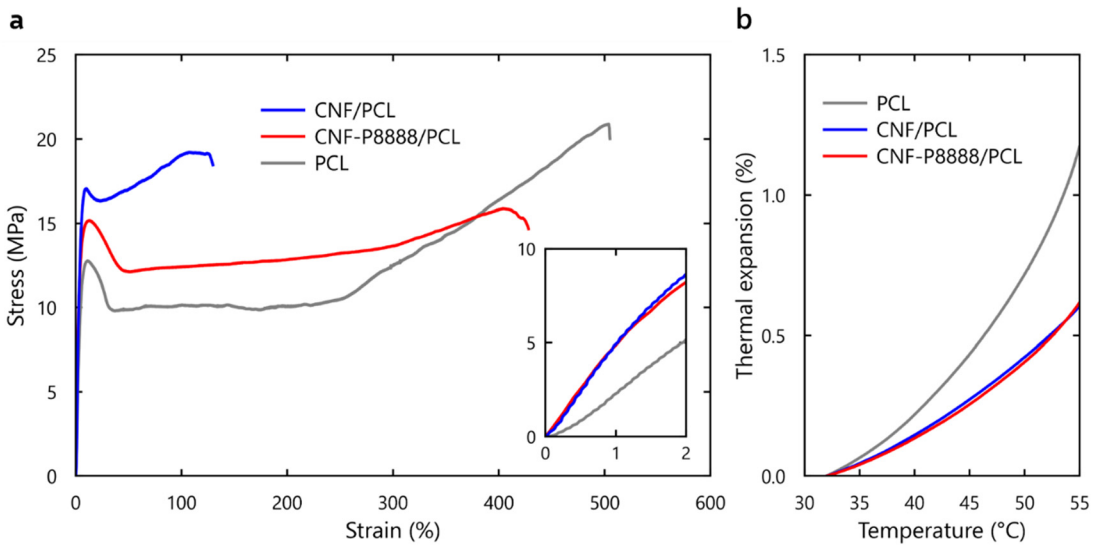

Fig. 3 Comparison of the reinforcing function between CNF-P8888 and pristine CNF. (a) Typical stress–strain curves and (b) thermal expansion curves of pristine PCL, CNF-P8888/PCL, and CNF/PCL at a 10% w/w CNF content.

of the CNF-P8888/PCL composite under the same content. However, the elongation at break of the CNF/PCL composite significantly decreased to 247%, resulting in a reduction in the toughness to 47 MJ m^{-3} (Table 1). Compared with matrix polymers, this embrittlement of composites is often observed for CNF-reinforced plastics produced *via* melt kneading.[22–25] It is thus significant that the toughness of surface-modified CNF-P8888/PCL was maintained while the modulus and strength increased.

Fig. 3b shows the thermal expansion behaviour of these composites. The coefficients of thermal expansion (CTEs) of PCL, CNF-P8888/PCL and CNF/PCL within the temperature range of 30–55 °C before the melting point of approximately 60 °C were 511, 268, and 264 ppm K^{-1}, respectively. The CTE values of the composites with CNF-P8888 and pristine CNF were nearly equivalent and were reduced by approximately half compared with the value of the PCL matrix alone.

A series of results demonstrated that CNF-P8888 is an excellent reinforcing filler for PCL that enhances the modulus and strength while preserving the toughness and, in addition, reduces the CTE.

Fig. 4a shows X-ray diffraction (XRD) profiles of pristine PCL, CNF/PCL and CNF-P8888/PCL at a 10% CNF content in the PCL matrix. These profiles were collected by the reflection mode (see Experimental method in SI). Sharp peaks at 2θ = values of 21.2° and 23.6° were observed for all the samples, corresponding to the (1 1 0) and (2 0 0) planes of orthorhombic PCL crystals.[32] No peaks due to crystalline CNFs were observed in either the CNF/PCL or CNF-P8888/PCL composites, probably because of the low CNF content. Moreover, compounding pristine CNF or CNF-P8888 with PCL significantly decreased the peak intensity of the (1 1 0) plane and slightly increased the peak intensity of the (2 0 0) plane compared with those of pristine PCL. The crystallite sizes along the directions perpendicular to the (1 0 0) and (2 0 0) planes calculated from the profiles using the Scherrer equation[33] are summarized in Table 2. The crystallite sizes of both the (1 1 0) and (2 0 0) planes slightly increased through the compounding of CNF and CNF-P8888, and the increase in the (2 0 0) plane was relatively significant compared with the (1 1 0) plane. Additionally, compared with CNF-P8888, the compounding of CNFs was more effective at increasing the crystallite sizes.

Fig. 4b shows differential scanning calorimetry (DSC) curves of the same samples. Endothermic reactions of PCL were observed within the temperature range of 35–55 °C, and the melting points of PCL, CNF/PCL, and CNF-P8888/PCL were 54.2 °C, 54.5 °C, and 53.2 °C, respectively, without significant differences among the samples. The degree of crystallinity (X_c) was calculated as follows:[34]

$$X_c(\%) = \frac{\Delta H_m}{\omega \times \Delta H_f} \times 100 \quad (1)$$

where ΔH_m, ΔH_f and ω are the melting enthalpy determined by DSC analysis, the melting enthalpy of a perfect PCL crystal (139.5 J g^{-1}),[35] and the weight fraction of PCL in the sample, respectively. The X_c values of PCL, CNF/PCL, and CNF-P8888/PCL

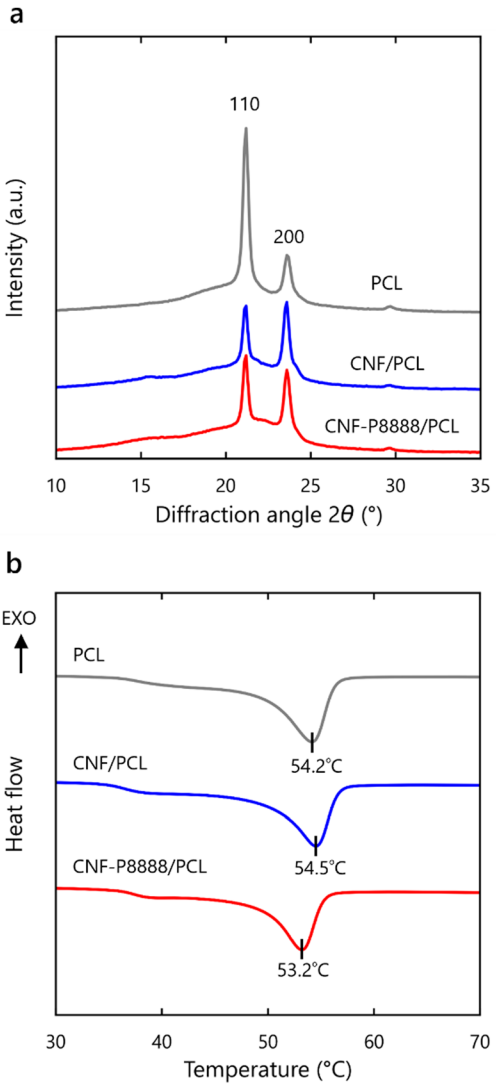

Fig. 4 Crystallinity analyses. (a) XRD profiles and (b) DSC curves of pristine PCL, CNF-P8888/PCL, and CNF/PCL at 10% w/w CNF content.

were approximately 45%, 45%, and 44%, respectively (Table 2), and were almost equivalent.

Crystallinity analysis revealed that combining CNF-P8888 with PCL did not significantly affect the crystallite size or degree of crystallinity of PCL, indicating that the enhancement in the mechanical properties of the CNF-P8888/PCL composites was due to the reinforcing effect of CNF-P8888. Moreover, considering the obvious decrease in the XRD intensity of the

Table 2 Structural properties of the pristine PCL, CNF-P8888/PCL, and CNF/PCL

Sample	CNF content (% w/w)	Density (g cm^{-3})	Crystallite size (nm)		Degree of crystallinity (%)
			1 1 0	2 0 0	
PCL	0	1.14	22.2	17.2	45
CNF-P8888/PCL	10	1.19	22.4	18.2	45
CNF/PCL	10	1.19	22.8	20.1	44

(1 1 0) plane, the planar orientation of the PCL crystallites facing the (1 1 0) plane parallel to the sheet surface of the pristine PCL was disturbed by the addition of CNFs.

The CNF-P8888 and pristine CNF fractions disintegrated in the kneading process were extracted from both the CNF-P8888/PCL and CNF/PCL composites, respectively, by dissolution of the PCL matrix in tetrahydrofuran. Fig. 5a–c show the fibre morphologies of TOP-P8888 before direct kneading, CNF-P8888, and pristine CNFs, respectively, as observed by scanning electron microscopy (SEM). After kneading, most of the coarse fibres of TOP-P8888 pulp disintegrated into CNF-P8888 with widths smaller than 1 μm (Fig. 5a and b). The pristine CNF fraction extracted from the CNF/PCL composites also exhibited widths smaller than 1 μm according to the SEM observations (Fig. 5c). However, a distinct difference in fibre morphology between the cellulose fractions within the CNF-P8888/PCL and CNF/PCL composites was detected *via* X-ray computed tomography (CT) analysis (Fig. 5d and e). The resolution of X-ray CT analysis in this study was 1 μm, and PCL exhibits a lower coefficient of X-ray absorption than cellulose does. Thus, the coloured parts in panels d and e in Fig. 5 represent the fibrous cellulose fractions with widths greater than 1 μm. In CNF-P8888/PCL (Fig. 5d), fibres were almost undetectable, indicating that the majority of the coarse fibres disintegrated into submicron-sized fibrils in the PCL matrix. In contrast, undisintegrated coarse fibres or aggregated fibrils were clearly observed in the CNF/PCL composites (Fig. 5e). This undisintegrated nature of the starting kraft pulp, without modifications *via* TEMPO-oxidation and P8888 bearing, explains the embrittlement of the CNF/PCL composite (Fig. 3). Notably, in the mechanics of composites, coarse foreign objects in a continuous phase induce stress concentrations during deformation.[26]

These results demonstrate that the thermo-softening nature of TOP-P8888 enhances the degree of fibrillation and dispersibility of CNFs in a polymer matrix through the process of direct kneading, which avoids stress concentration, resulting in the high toughness of the CNF-P8888/PCL composites.

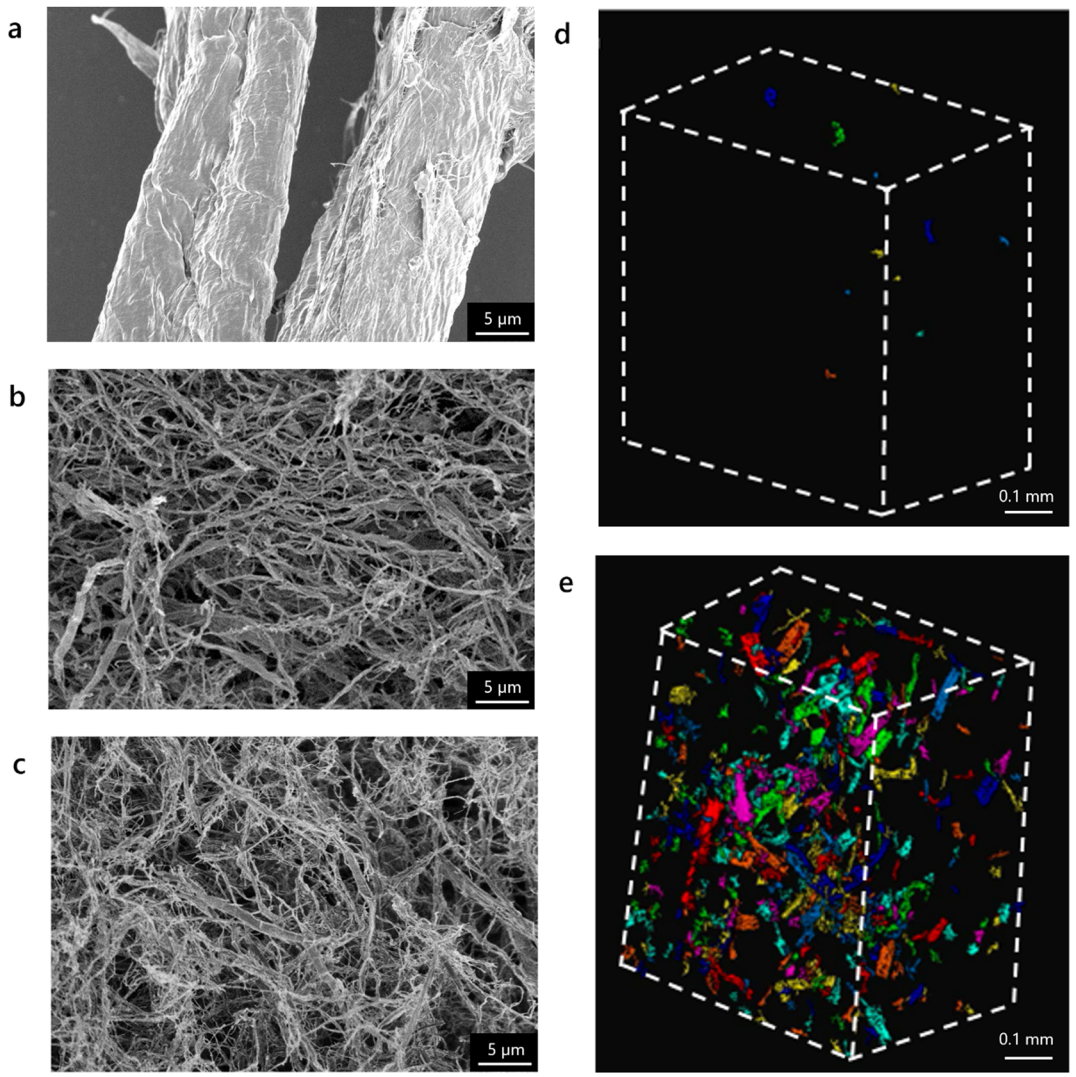

Fig. 5 Fibre morphology. SEM images of (a) TOP-P8888, (b) CNF-P8888, and (c) pristine CNF. X-ray CT images of (d) CNF-P8888/PCL and (e) CNF/PCL composites at 10% w/w CNF content.

Conclusions

We fabricated tough CNF-reinforced PCL composites *via* the direct kneading of thermo-softening pulp. Thermo-softening pulp was prepared by introducing $P8888^+$ as the carboxylate counterion in TOP and then disintegrated into CNF-P8888 in a PCL matrix.

The compounding of CNF-P8888 with a 2% CNF content increased all the tensile properties of PCL or its Young's modulus, yield strength, elongation at break, and toughness (mechanical energy required until break). Young's modulus and the yield strength of the CNF-P8888/PCL composites increased with increasing CNF content. At a 10% CNF content, these two properties were enhanced by 70% and 20%, respectively, compared with the original PCL properties, while the toughness was preserved. In contrast, the elongation at break of the unmodified CNF/PCL composite at a 10% CNF content significantly decreased, resulting in a reduction in toughness. The CTE values of the CNF-P8888/PCL and unmodified CNF/PCL composites at a 10% CNF content were nearly equivalent and decreased by approximately half of the CTE of the pristine PCL. The addition of CNF-P8888 to PCL did not significantly affect the crystallite sizes and the degree of crystallinity of PCL. SEM and X-ray CT analyses of the composites revealed that most of the coarse fibres of TOP-P8888 pulp disintegrated into CNF-P8888 with nanoscale widths and were uniformly dispersed in the PCL matrix, which should have contributed to the high toughness of the CNF-P8888/PCL composites.

This study demonstrated that the mechanical strength and thermal dimensional stability of PCL can be enhanced while maintaining toughness *via* energy- and time-saving direct kneading of thermo-softening pulp with PCL. This strategy is industrially feasible because of its low cost and environmental friendliness. Additionally, this strategy can be applied to other polymers, expanding the use of sustainable wood-derived CNFs.

Author contributions

Masahiro Kasamatsu: writing – original draft, visualization, investigation, formal analysis, and data curation. Shun, Ishioka: writing – original draft, methodology, formal analysis, and funding acquisition. Noriyuki Isobe: writing – review and editing, formal analysis, and funding acquisition. Katsunori Kimoto: writing – review and editing, formal analysis, and data curation. Satoshi Okada: writing – review and editing, formal analysis, and data curation. Yohsuke Goi: writing – review and editing and resources. Shuji Fujisawa: writing – review and editing, formal analysis, and funding acquisition. Tsuguyuki Saito: writing – review and editing, supervision, methodology, funding acquisition, and conceptualization.

Conflicts of interest

There are no conflicts to declare.

Data availability

Data for this article are available at the figshare at **https://doi.org/10.6084/m9.figshare.28792334.v3**.

Supplementary information is available. See DOI: **https://doi.org/10.1039/d5nh00271k**

Acknowledgements

This work was in part supported by the JST CREST program (JPMJCR22L3), the JST ASPIRE program (JPMJAP2310), the JSPS Grant-in-Aids for Scientific Research (23K26963; 23H02270; 23K25040), and the Asahi Woodtec Foundation (24-II-05).

References

1 H. Kargarzadeh, M. Mariano, J. Huang, N. Lin, I. Ahmad, A. Dufresne and S. Thomas, *Polymer*, 2017, **132**, 368–393.
2 S. Fujisawa, T. Ikeuchi, M. Takeuchi, T. Saito and A. Isogai, *Biomacromolecules*, 2012, **13**, 2188–2194.
3 J. N. Coleman, U. Khan, W. J. Blau and Y. K. Gun'ko, *Carbon*, 2006, **44**, 1624–1652.
4 J. N. Coleman, U. Khan and Y. K. Gun'ko, *Adv. Mater.*, 2006, **18**, 689–706.
5 M. T. Byrne and Y. K. Guin'Ko, *Adv. Mater.*, 2010, **22**, 1672–1688.
6 A. Okada and A. Usuki, *Macromol. Mater. Eng.*, 2006, **291**, 1449–1476.
7 M. Triaki, A. Benmounah and A. Zenati, *Polym. Bull.*, 2021, **78**, 3275–3292.
8 F. Guo, S. Aryana, Y. Han and Y. Jiao, *Appl. Sci.*, 2018, **8**, 1696.
9 K. I. Winey and R. A. Vaia, *MRS Bull.*, 2007, **32**, 314–322.
10 V. Shah, J. Bhaliya, G. M. Patel and K. Deshmukh, *Polym. Adv. Technol.*, 2022, **33**, 3023–3048.
11 Q. Wang and L. Zhu, *J. Polym. Sci., Part B: Polym. Phys.*, 2011, **49**, 1421–1429.
12 D. Feldman, *J. Macromol. Sci., Part A: Pure Appl. Chem.*, 2014, **51**, 203–209.
13 I. Sakurada, Y. Nukushina and T. Ito, *J. Polym. Sci.*, 1962, **57**, 651–660.
14 T. Saito, R. Kuramae, J. Wohlert, L. A. Berglund and A. Isogai, *Biomacromolecules*, 2013, **14**, 248–253.
15 R. Hori and M. Wada, *Cellulose*, 2005, **12**, 479–484.
16 K. Daicho, S. Fujisawa and T. Saito, *Biomacromolecules*, 2023, **24**(2), 661–666.
17 Y. Nishiyama, *J. Wood Sci.*, 2009, **55**, 241–249.
18 A. Abdulkhani, J. Hosseinzadeh, A. Ashori, S. Dadashi and Z. Takzare, *Polym. Test.*, 2014, **35**, 73–79.
19 C. M. Wu, K. S. Danh and A. N. Nakagaito, *Exp. Polym. Lett.*, 2020, **14**, 467–476.
20 K. Choo, Y. C. Ching, C. H. Chuah, S. Julai and N. S. Liou, *Materials*, 2016, **9**, 644.
21 W. Sakuma, S. Fujisawa, L. A. Berglund and T. Saito, *Nanomaterials*, 2021, **11**, 3032.
22 Y. Igarashi, A. Sato, H. Okumura, F. Nakatsubo and H. Yano, *Chem. Eng. J.*, 2018, **354**, 563–568.

23 K. Sakakibara, Y. Moriki and Y. Tsujii, *ACS Appl. Polym. Mater.*, 2019, **1**, 178–187.
24 Y. Igarashi, A. Sato, H. Okumura, F. Nakatsubo, T. Kuboki and H. Yano, *Cellulose*, 2022, **29**, 2985–2998.
25 T. Semba, A. Ito, K. Kitagawa, H. Kataoka, F. Nakatsubo, T. Kuboki and H. Yano, *Composites, Part A*, 2021, **145**, 106385.
26 N. Herrera, P. Olsén and L. A. Berglund, *ACS Sustainable Chem. Eng.*, 2020, **8**, 11977–11985.
27 S. Ishioka, Y. Hiromatsu, J. Peng, T. Kabe, T. Kasuga, K. Daicho, Y. Goi, N. Isobe, T. Yamaguchi, S. Fujisawa, H. Koga, T. Iwata, J. Shiomi, M. Nogi and T. Saito, *ChemRxiv*, 2025, preprint, DOI: **10.26434/chemrxiv-2025-ljf83**.
28 S. Chen, D. Zhao, J. Zhu, J. Wang, G. Zhong, H. Huang and Z. Li, *SusMat*, 2024, **4**, e238.
29 S. Thangavel, K. T. Kandasamy, R. Rathanasamy and R. Dhairiyasamy, *Rev. Mater.*, 2024, **29**, e20240324.
30 T. Saito, S. Kimura, Y. Nishiyama and A. Isogai, *Biomacromolecules*, 2007, **8**, 2485–2491.
31 V. Abhijit, T. Johannes, K. Sahlin-Sjövold, R. Mikael and A. Boldizar, *Polym. Eng. Sci.*, 2020, **60**, 956–967.
32 R. Balu, T. S. Sampath Kumar, M. Ramalingam and S. Ramakrishna, *J. Biomater. Tissue Eng.*, 2011, **1**, 30–39.
33 M. A. Adamu, M. Sumaila, M. Dauda and T. Ause, *Sci. Afr.*, 2023, **19**, e01563.
34 P. V. Joseph, K. Joseph, S. Thomas, C. K. S. Pillai, V. S. Prasad, G. Groeninckx and M. Sarkissova, *Composites, Part A*, 2003, **34**, 253–266.
35 I. Castilla-Cortázar, A. Vidaurre, B. Marí and A. J. Campillo-Fernández, *Polymers*, 2019, **11**, 1099.